© 2018 IJSRSET | Volume 4 | Issue 11 | Print ISSN: 2395-1990 | Online ISSN : 2394-4099
Themed Section : Engineering and Technology
DOI : https://doi.org/10.32628/IJSRSET11841129

Synthesis and Characterization of Onion Mediated Silver Doped Zinc Oxide Nanoparticles

N. Tensingh Baliah, P. Muthulakshmi, S. Lega Priyatharsini

Center for Research And Post Graduate Studies In Botany, Ayya Nadar Janaki Ammal College, Sivakasi, Tamil Nadu, India

ABSTRACT

Green synthesis of nanoparticles has attracted considerable attention in recent years. In this regard, plants extracts and natural resources such as microorganisms and enzymes have been found to be good alternative reagents in nanoparticles synthesis. Utilizing green substances has several advantages including low energy consumption and moderate operation conditions without using any toxic chemicals. An attempt was made to synthesis and characterizes the silver doped zinc oxide nanoparticles (Ag doped ZnO NPs) by using onion extract. The synthesized Ag doped ZnO NPs were characterized by Scanning Electron Microscopy (SEM), Energy Dispersive X-ray Spectroscopy Analysis (EDAX), Fourier Transform Infrared Spectroscopy (FTIR), X-Ray Diffraction (XRD) and Zeta potential analyses. These characterizations revealed that doped nanoparticles are differed in their structural properties. The onion extract was used as reducing agent as well as stabilizer. The phytochemicals found in the onion extract were responsible for the formation of Ag doped ZnO NPs.

Keywords : Nanoparticles, Onion, Silver Nitrate, Zinc Oxide, Doped

I. INTRODUCTION

Synthesis of nanoparticles is gigantic and an expanding area due to their potential applicability in numerous fields such as electronics, optoelectronics, functional biology, drug delivery, antimicrobial and biosensors [1]. There are various methods of synthesizing nanoparticles such as ultraviolet irradiation, aerosol technologies, lithography, laser ablation, ultrasonic fields, heating and electrochemical reduction, photochemical reduction [2] but these techniques are expensive and sometimes hazardous chemicals are involved in their synthesis which is harmful to the environment also [3].

There is a need to develop environment friendly procedures for synthesis of nanoparticles through "green synthesis". To circumvent this many biological systems like bacteria, fungi, yeast, cyanobacteria, actinomycetes and plants have been used. But the best one appears to be the use of plants [4], [5]. Biological methods are better methods due to slower kinetics, better manipulation and control over crystal growth and stabilization [6]. Plants have the ability to reduce metal ions much faster as compared to microorganisms and synthesize stable metal nanoparticles. When plants are used as the biomaterials for the synthesis of nanoparticles, the protocol provides the way to change the shape and size of the nanoparticles by simple altering the pH [7]. Among the several noble metal nanoparticles, silver nanoparticles (Ag NPs) are having special attention due to their unique properties including appropriate electrical conductivity, chemical stability, catalytic and antimicrobial activities [8]. Highly ionic nanoparticulate metal oxides such as zinc oxide nanoparticles (ZnO NPs) are unique in that they can be produced with high surface areas and with unusual crystal structures. Compared to organic materials,

inorganic materials such as ZnO possess superior durability, greater selectivity and heat resistance [9].

In Ag doped ZnO NPs, the diffusion of Ag into ZnO could cause variation in its lattice structure. Ag could be a good candidate to improve luminescence efficiency. The silver doping into ZnO influenced the absorption, visible emission and the corresponding transitions of electron and excitons in ZnO host lattice [10]. The zinc oxide flower like structures have 20 nm diameter and 200 nm length while the synthesized nickel doped ZnO NPs were having 50 nm size. These sizes match with that of calculated by Debye Scherrer formula. SEM studies provided further insight into the morphology and size details of the ZnO nanoparticle [11].

II. MATERIALS AND METHODS

A. Preparation of onion extract

The onion bulbs were washed with sterile distilled water. The outer covering of the bulb was manually peeled off and the fleshy part of the onion was rewashed with sterile distilled water. A part of 10 g of the onion bulb was cut into small pieces and ground using with distilled water and filtered using muslin cloth and then Whatmann No.1 filter paper. The filtrate was used as reducing agent and stabilizer. Silver nitrate and zinc nitrate (1mM) was used as precursor for the synthesis of silver doped zinc oxide nanoparticles. These solutions were prepared as fresh.

B. Synthesis of silver doped zinc oxide nanoparticles (Ag doped ZnO NPs)

Ag doped ZnO NPs were synthesized by the method followed by [12]. For the synthesis of silver doped zinc oxide nanoparticles, 10ml of onion aqueous extract was mixed with 90 ml of each 1mM silver nitrate and zinc nitrate solution. The content was incubated at room temperature for 24 hours. After the incubation period, the content was centrifuged at 10,000rpm for 20 minutes. The pellet was collected and dried at 90°C for 6-8 hours. The powder obtained was carefully collected and packed for characterization purpose.

C. Recovery and Characterization of nanoparticles

The nanoparticles thus obtained were purified by repeated centrifugation at 10000 rpm at 25°C for 10minutes. It was followed by re-dispersion of the pellet in deionized water to get rid of any uncoordinated biological molecules. The process of centrifugation and re-dispersion were repeated with sterile distilled water to ensure better separation of free entities from the nanoparticles. The synthesized nanoparticles were characterized by UV-Visible spectroscopy, Scanning Electron Microscopy (SEM), Energy Dispersive X-ray Spectroscopy Analysis (EDAX), Fourier Transform Infrared Spectroscopy (FTIR), X-Ray Diffraction (XRD) and Zeta potential analyses.

D. UV-Visible Spectroscopy analysis

The reduction of pure metal ions was confirmed by measuring the absorption of reaction mixture by UV-Vis Spectrophotometer (UV 1700 SHIMADZU) from 200 to 800 nm [13].

E. Fourier Transform Infrared (FTIR) analysis

FTIR has become an important tool for understanding the involvement of functional groups in interactions between metal particles and biomolecules. FT-IR spectra were recorded at 1 cm^{-1} resolution by FTIR spectrophotometer (FTIR-8400S SHIMADZU) using KBr pellet technique [14].

F. X-Ray Diffraction (XRD) analysis

To determine the nature and size of the synthesized nanoparticles, X-ray diffraction (XRD) was performed. The pellet was dissolved in deionized sterile water and washed thrice in the same by centrifugation. The pellet was retained and air dried. The powder from of the sample was coated on the XRD grid, the spectra were recorded 40 kV and a current of 30 mA with CuKα radiation using XRD (Philips PW1050/37 model). The diffracted intensities were recorded from 20°C to 80°at 2θ angles. The crystalline nature of

synthesized nanoparticles was calculated from the width of the XRD peaks, using the Debye- Scherrer formula ($D= K\lambda/\beta \cos\theta$).

H. Scanning Electron Microscopy (SEM) analysis

The synthesized nanoparticles were dispersed in water and the resultant suspensions were homogenized using ultra sonicator for one to two hours. A drop of the nanoparticles suspension was placed on a piece of micro glass slide attached to a metal grid coated with carbon film, and dried it gradually at room temperature. The sample was then sputter coated with gold and visualized with a JEOL JSM-6480 LV SEM to assess the particle size, shape and percentage [15].

I. Energy Dispersive X-Ray Spectroscopy (EDAX) analysis

A drop of the nanoparticles suspension was placed on a piece of microglasws slide attached to a metal grid coated with carbon film, and dried it gradually at room temperature. X-ray spectrometer (EDAX) operated at an accelerating voltage at 10 KeV. The sample was then sputter coated with gold and visualized with a BRUKER to assess the particle size, shape and percentage of synthesized particles.

J. Zeta Potential analysis

The supernatant was filtered and then sonicated for 5 minutes. The solution was centrifuged for 15 minutes at 25°C with 5000 rpm and the supernatant was collected. Then, the supernatant was diluted for 4 to 5 times and then set for Zeta-Potential analysis [16].

III. RESULTS AND DISCUSSION

A. VISUAL OBSERVATION OF NANOPARTICLES

The synthesized nanoparticles were initially confirmed by visual observation by colour change. The metal ions were reduced during the exposure to aqueous extract of onion within 24 hours of incubation period. It was observed that the colour of the reaction mixture was changed for silver doped zinc oxide to pale yellow to dark brown (Fig.1).

A B C

Fig. 1: Visual observation of Ag Doped ZnO NPs A-Onion B-$AgNO_3$ and Zn $(NO_3)_2$ C- Ag doped ZnO NPs

B. UV-VISIBLE SPECTROSCOPY ANALYSIS

The reduction of metal ions in the onion extract was further confirmed by UV-Vis Spectrophotometer. UV-Vis absorption spectra of nanoparticles were shown in Fig. 2. The absorption spectra of Ag doped ZnO nanoparticles formed in the reaction media has absorbance maximum at 472nm. UV-Vis absorption spectra of the ZnO and Ag doped ZnO were observed. Absorption edge for ZnO and Ag doped ZnO were observed at 376 and 416nm respectively. This absorption peak was red shifted, as compared to the bulk exciton, which was due to the size effect of the nanostructures. Ag-doped ZnO showed red shift in the absorption edge compared to pure ZnO. This may be due to creation of localized energy levels by doped Ag in the band gap of ZnO. Therefore, optical absorption edge of the catalyst Ag doped ZnO obviously shifted further to the visible region and a significant enhancement of the visible-light absorption is obvious. Thus, the improvement of the visible-light absorption can be attributed to the presence of metallic Ag that contributes to the narrowing of band gap of ZnO [17] by extending its absorption edge to the visible region to harvesting more photons.

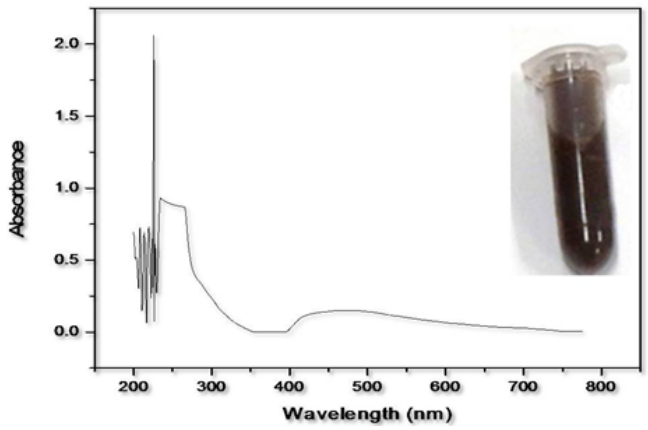

Fig. 2 : UV-Visible Spectrum of Ag Doped ZnO NPs

The UV–Vis spectra of the Ag NPs and ZnO and Ag-ZnO nanostructures were measured with the Perkin-Elmer spectrophotometer and the overall spectral range of 300–900nm. The absorbance spectrum of the Ag-ZnO nanostructures has a typical surface plasmon resonance (SPR) peak at approximately 440nm, indicated the presence of $Ag^{(0)}$ NPs on the ZnO surface. Previous studies have reported that Ag NPs 10–50 nm in size that were embedded in ZnO nanostructures cause intense photon scattering, which was responsible for the increased photocatalytic activity in direct light. The surface plasmon band in the Ag-ZnO nanostructures has slightly broadened, showing a red shift compared to that of pure Ag, which might be due to the strong interfacial electronic coupling between the neighboring ZnO and Ag NPs [18].

C. FOURIER TRANSFORM INFRARED SPECTROSCOPY (FTIR) ANALYSIS

FTIR analysis is unique for the identification of various functional groups and to identify the biomolecules which were responsible for the reduction of metal ions into nanoparticles in the presence of onion extract (Fig. 3). The phytochemical found in the onion extract were responsible for the formation of various nanoparticles. The FT-IR spectrum of onion extract showed several absorption peaks ranged from 3421cm^{-1} to 677 cm^{-1}. The region of band was phenols, alkanes due to N-H Stretching of proteins and O-H stretching, > C=O stretching of esters, aromatics, ring C-C stretching of phenyl, alkanes, C-O stretch in vibration combined with the ring stretch of phenyl, Aliphatic amines, alcohols, Carboxylic acids, ester, ether, Functional groups mainly from Carbohydrate, alkyl halides (Table 1). FT-IR measurement for the silver doped Zinc oxide nanoparticles indicated that presence of peaks at 32.89.37cm^{-1}, 1655.77cm^{-1}, 1627.81cm^{-1}, 1534.27cm^{-1}, 1383.83cm^{-1}, 1357.79cm^{-1}, 1010.63cm^{-1} and 535.21cm^{-1}. Those peaks were assigned to the O-H stretching and bending, -H-O-H bending vibration mode, C=O and O-H bending vibrations, -C=O or O-H, oxygen stretching and bending frequency and metal oxide bond (Table 2).

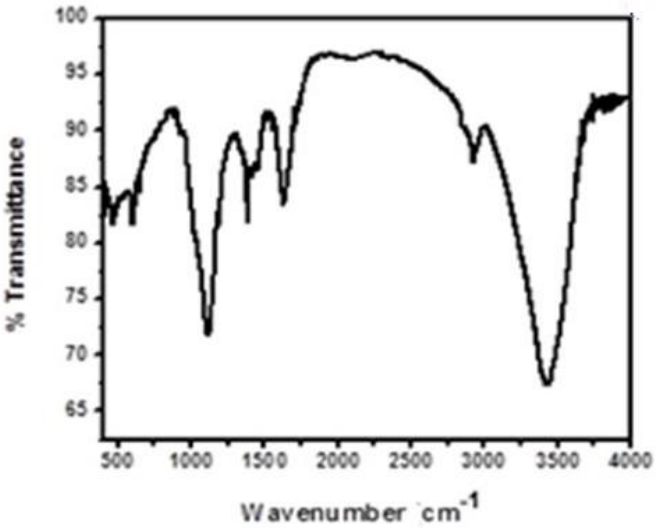

Fig 3: FTIR spectrum of Ag Doped ZnO NPs

Pure ZnO and Ag doped ZnO possess wurtzite structure and were further supported by FTIR spectra. The FTIR spectra of ZnO and ZnO:Ag nanoparticles were recorded in the range 500 – 4000 cm^{-1}. The characteristic stretching modes of Zn-O and Ag-O bonds were assigned to the significant bands at 479 and 538 cm^{-1}. The peak at 1036 and 1029 cm^{-1} were attributed to aromatic C=C stretching mode. The absorption bands at 3459 and 3478 cm^{-1}arise due to the stretching mode of O-H group which revealed the

existence of small amount of water absorbed by the ZnO nanostructure. The peaks located at 2358 and 2368cm^{-1} were due to the atmospheric CO_2 present in the instrument. The band at 2915 and 2928cm^{-1}were attributed to C-H stretching vibrations. The peak shift observed around 479 cm^{-1}to higher wave number 538 cm^{-1}indicated the Ag doping into the ZnO host lattice [19].

Table 1: Interpretation of FTIR spectrum analysis for onion extract

S. No.	Peak value (cm^{-1})	Interpretation
1	3421.48	Phenols
2	2926.78	Alkanes due to N-H stretching
3	1719.42	C=O stretching of Esters
4	1659.63	Aromatics
5	1627.81	C-C stretching vibration combined with Phenyl ring
6	1449.49	C-H Alkanes
7	1383.83	C-O stretching vibration combined with Phenyl ring
8	1071.38	Aliphatic Amines, Carboxylic acids, Ester, Ether
9	923.84	Carbohydrate
10	784.01	Alkyl halides
11	677.93	Alkyl halides

The FTIR spectra for pure and doped ZnO samples showed that there were broad peaks at 3450 and 1630 cm^{-1}, corresponding to the surface-adsorbed water and hydroxyl groups, respectively. The strong peak at 500 cm^{-1} was assigned to the characteristic of ZnO. FTIR spectra also showed numerous vibrational modes at low frequency which could be attributed to the different group frequencies of residual group and reaction byproducts. No vibrations in relation with Ag were detected in doped ZnO samples, indicating that there is no chemical bonding between Ag and ZnO [20].

Table 2: Interpretation of FTIR spectrum analysis for Ag Doped ZnO NPs

S. No.	Peak value (cm^{-1})	Interpretation
1	3289.37	O-H Stretching
2	1655.77	H-O-H bending vibration mode
3	1627.81	H-O-H bending vibration mode
4	1534.27	C=O & O-H bending vibration
5	1383.83	Asymmetric and Symmetric stretching of acetate
6	1357.79	C=O & O-H
7	1010.63	Oxygen Stretching & bending
8	535.21	Metal Oxide bond

D. X-RAY DIFFRACTION (XRD) ANALYSIS

The green synthesized nanoparticles using onion extract were further confirmed by the characteristic peaks observed in XRD analysis (Fig. 4). The various peaks in the XRD pattern could be assigned to the crystalline zinc oxide phase with the hexagonal wurzite structure with the lattice parameters a=5.2042 nm and c= 5.2075 nm. The XRD pattern showed different intensity peaks in the whole spectrum of 2θ values ranging from 20° to 80° for the onion. The onion extract mediated synthesized silver nanoparticles, as evident from the peaks at 2θ values of 32.53°, 38.25°, 44.43°, 46.46° and 64.72°, corresponding to Ag(311), Ag(111), Ag(200), (420) and (222) planes respectively. The average crystalline size was determined using Scherrer's equation. The onion mediated Ag doped ZnO nanostructure was confirmed by the characteristic peaks observed in the XRD analysis. The peaks in the XRD pattern could be assigned to the crystalline zinc oxide phase with the

hexagonal wurzite structure with the lattice parameters a=5.558 nm and c= 3.230 nm. The diffraction lines observed at 2θ angle 27.54, 32.09, 46.09, 54.80, 57.27, 67.30 and 76.59° were indexed as (001), (101), (121), (221), (301), (400) and (141) respectively. The average size of the Ag-ZnO nanoparticles found to be 25 nm.

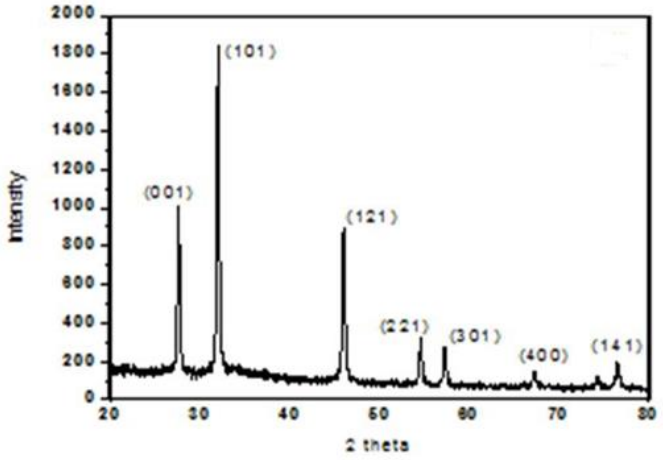

Fig. 4: XRD spectrum of Ag Doped ZnO NPs

For the Ag-doped and undoped ZnO were analyzed by XRD. The diffraction peaks could be readily indexed as wurtzite type ZnO (hexagonal structure; JCPDS: 36–1451) for both pure and Ag-doped ZnO samples, which was accorded well with the reported data (JCPDS File No. 36–1451). The peaks at 2θ of 31.8°, 34.5°, 36.3°, 47.6° and 56.5°, correspond to the crystal planes (100), (002), (101), (102), and (110) of crystalline ZnO, respectively. However, no such shift in the peak positions or diffraction peaks from any other chemical species, such as silver and/or silver oxide, was observed in any of the modified samples, which might be ascribed to a low amount, the amorphous state or the high dispersion of Ag [21].

XRD patterns of the pure ZnO and Ag-ZnO nanostructures were analyzed. The peaks of a typical ZnO hexagonal wurtzite structure (JCPDS card no. 36-1451) were present in both XRD patterns. For the Ag-ZnO nanostructures, there were two mixed sets of diffraction peaks present. In addition to the ZnO peaks, the three additional peaks at 38.37°, 44.78° and 64.81° were assigned to a cubic Ag structure (JCPDS card no. 04-0783). It was also evident that there were no large shifts in the positions of the diffraction peaks, which further confirmed that the as-synthesized samples were composed of ZnO and Ag phases [22].

E. SCANNING ELECTRON MICROSCOPE (SEM) ANALYSIS

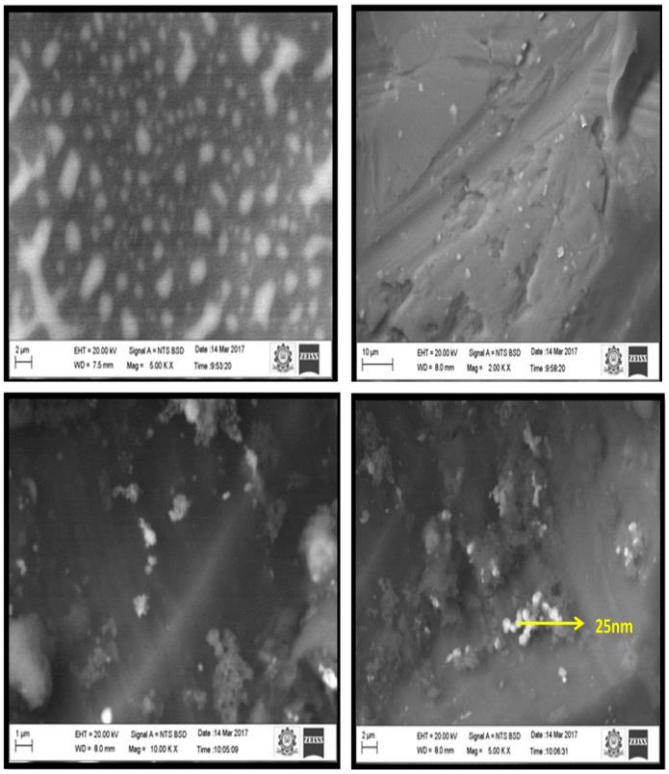

Fig. 5: SEM micrograph of Ag Doped ZnO NPs at different magnifications

The surface morphology of the nanoparticles were characterized using Scanning Electron Microscopy. From the SEM analysis, silver doped zinc oxide as cubic rocksalt in nature (Fig. 5). The typical SEM images were taken for the zinc tartrate precursor and Ag/ZnO composite. The zinc tartrate precursor was rod-like with an average diameter about 1 μm and a length up to 10 μm. It can be seen that the precursor morphology has been well retained and the surface became rough compared with the precursor. The microstructure of the doped nanoparticle was further investigated by TEM. The Ag/ZnO microrods consisted of plenty of nanocrystals. The nanocrystals were bound to each other to form porous structure.

The nanoholes with a size of several nanometers were also clearly found, which may greatly enhance the surface area of the sample [23]. Surface morphology of the synthesized doped nanoparticles was identified from SEM electron micrograph. The results revealed that the SEM micrographs of Ag doped ZnO nanoparticles were spherically in shaped [24]. The chemical composition of the Ag doped ZnO was obtained from EDAX spectrum. The elemental composition from the EDAX spectrum confirmed the presence of Zn, O and Ag in the sample.

F. ENERGY DISPERSIVE X-RAY SPECTROSCOPY (EDAX) ANALYSIS

EDAX analysis is very much useful for further confirmation of presence of nanoparticles. The EDAX analysis showed the confirmative peaks for Ag doped ZnO NPs by typical absorption peak at 3KeV and 1KeV respectively (Fig. 6).

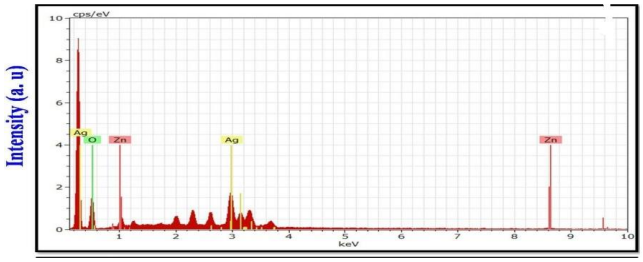

Fig.6: EDAX spectrum of Ag Doped ZnO NPs

A study on Cu and Ag doped ZnO nanoparticles showed the EDS of Ag (1–3%) doped and Cu (1–3%) doped ZnO NPs. EDAX analysis confirmed the presence of the dopant ions (Ag and Cu) in the Ag and Cu doped ZnO NPs. A trace amount of sulfur and carbon were present in all the samples which may result from the incomplete conversion of $ZnSO_4$ into $Zn(OH)_2$ and capping agent PVP, respectively [25]. In order to confirm the presence of Ce ion doped ZnO nanoparticles synthesized using *Sesbania grandiflora*, EDAX spectroscopy was performed. The EDAX spectrum of Ce ion doped zinc oxide nanoparticles synthesized using *Sesbania grandiflora* leaf extract. Ce ion doped zinc oxide nanoparticles were found to have atomic percentage 37.61 of Zn, 19.86 of O, 6.31 of Ce. This confirmed the doping of Ce ion in ZnO lattice.

The EDAX spectrums of the Ag doped PVP-ZnO nanofibers showed the presence of C, Zn, and O along with Ag peaks and the intensity of Ag peaks increase with increasing percentage of doping. The EDAX spectrum showed that the Zn-Ag material include elements such as Zn, O and Ag. The quality of Ag content deduced from the EDAX spectrum about 3% indicates that Ag particles were loosed in the reaction process [26]. The morphologies of Ag doped ZnO–PVP composite electrospun nanofibers were analyzed with EDAX spectrum. The results indicated that the Ag doped ZnO– PVP nanofibers contained the same morphology of parent ZnO–PVP nanofiber and there was no appraisable change in fiber diameter was observed. The surface of the nanofibers were not smooth due to presence of very fine Ag nanoparticles with particle diameters around 10-50 nm on the fiber surfaces. The EDAX spectra of the Ag doped PVP-ZnO nanofibers showed the presence of C, Zn, and O along with Ag peaks and the intensity of Ag peaks increase with increasing percentage of doping [27].

G. ZETA POTENTIAL

Zeta potential measures the potential stability of the nanoparticles in the colloidal suspension. From the Zeta potential analysis, onion extract mediated silver doped Zinc oxide nanoparticles carry a charge of ±28.0 mV. From this findings, the stability of the onion mediated synthesized nanoparticles have good stability (Fig. 7). The zeta potential used to determine the surface potential of the silver nanoparticles synthesized using *Urtica dioica* leaves extract. Zeta potential is an essential characterization of stability in aqueous silver nanoparticles. A minimum of ±30mV zeta potential was required for the indication of stable silver nanoparticles. For the obtained nanoparticles, zeta values were measured and found to be ±25.1mV with a peak area of 100% intensity. These values provided the full stabilization of the nanoparticles,

which may be the main reason in producing particle sizes with a narrow size distribution index [28].

The zeta potential of the biologically synthesized NPs was determined in water as dispersant. The zeta potential was found to be -20 to -30 and -25 to -35-mV for ZnO and CuO, respectively. The high negative value approved the repulsion among the particles and thereby increases in stability of the structure of NPs [29]. The zeta potential of the biosynthesized Ag NPs was found as a sharp peak at –7.66 mV. It was suggested that the surface of the nanoparticles was negatively charged and dispersed in the medium. The negative value confirms the repulsion among the particles and proves that they are very stable [30].

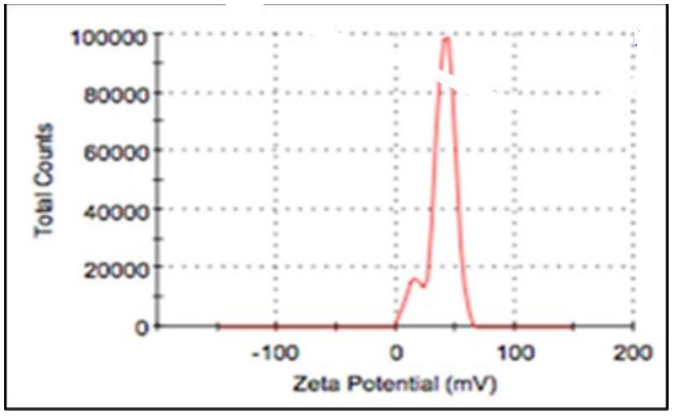

Fig.7: Zeta potential spectrum of Ag Doped ZnO NPs

IV. CONCLUSIONS

The adopted method is well suited with green chemistry principles as the plant extract serves as a dual functional molecule as reductant and a stabilizing agent for the synthesis nanoparticles. Zinc oxide nanomaterials are non-hazardous with wide band gap has been identified as a potential semiconducting material for exhibiting room temperature ferromagnetism when it is doped with transition metals like silver (Ag). Doping of transition metals into zinc oxide nanoparticles are well thought-out to be an efficient process to fine-tune the energy level structure of the host which can be further improved by the different concentrations of the dopants leading refining the optical properties. The modification of ZnO with noble metal (Ag) is found to be helpful way for preparation of highly active photocatalysts. Incorporating silver in ZnO is now an exciting area in research for developing electronic applications. Ag doped zinc oxide and Ag-N co-doped zinc oxide photocatalysts showed higher photocatalytic activity than undoped one.

V. ACKNOWLEDGEMENT

The authors are thankful to the Management and the Principal of Ayya Nadar Janaki Ammal College, Sivakasi, Tamil Nadu, India for providing laboratory facilities to carry out the experiment.

VI. REFERENCES

[1]. K Kavitha, S. Baker, D. Rakshith, H. Kavitha, B. Harini and S. Satish, “Plants as green source towards synthesis of nanoparticles,” Int. Res. J. Biol. Sci. vol. 2, pp. 66-76, 2013.

[2]. L Christensen, S. Vivekanandhan, M. Misra, A. Mohanty, “Biosynthesis of silver nanoparticles using Murraya koenigii (curry leaf) an investigation on the effect bof broth concentration in reduction mechanism and particle size,” Adv. Mat. Lett.vol. 2, pp. 429-434, 2011.

[3]. K C. Grabar, R. G. Freeman, M. B. Hommer and M. J. Natan, “Preparation and characterization of Au colloid monolayers,” Anal. Chem. vol. 67, pp. 735-743, 1995.

[4]. A Z. Mirza and H. Shamshad, “Preparation and characterization of doxorubicin functionalized gold nanoparticles, “Eur. J. Med. Chem. vol. 46, pp. 1857-1860, 2011.

[5]. A K. Singh, M. Talat, D. Singh, P. Srivastava, “Biosynthesis of gold and silver nanoparticles by natural precursor clove and their

functionalization with amine," J. Nanopart. Res. vol. 12, pp. 1667-1675, 2010.

[6]. B S. Nayak, S. S. Raju, F. A. Orette and A. V. C. Rao, "Effects of Hibiscus rosasinensis L. (Malvaceae) on wound healing activity: a preclinical study in a sprague dawley rat.," Int. J. Lower Extremity Wounds, Vol. 6 no. 2, pp. 76-81, 2007.

[7]. J L. Gardea-Torresdey, E. Gomez, J. R. Peralta-Videa, J. G. Parsons, H. Troiani and M. Jose Yacaman, "Alfalfa sprouts: a natural source for the synthesis of silver nanoparticles," Langmuir, vol. 19, pp. 1357–1361, 2003.

[8]. V Vijayakumar and A. K. Kumaraguru, "Antibacterial potential of biosynthesised silver nanoparticles using Avicennia marina mangrove plant," Appl. Nanosci. vol. 2, pp. 143-147, 2012.

[9]. N Padmavathy and R. Vijayaraghavan, "Enhanced bioactivity of ZnO nanoparticles - An antimicrobial study," Sci. Technol. Adv. Mater. vol. 9. pp. 432-438, 2008.

[10]. A. M. Oztas, M. L. Smith and J. Paul, "Spacetime curvature is important for cosmology constrained with supernova emissions," Int. J. Theoret. Phys. vol. 47, pp. 725-740, 2008.

[11]. D. Gnanasangeetha and S. D. Thambavani, "One pot synthesis of zinc oxide nanoparticles via chemical and green method," Res. J. Mat. Sci. vol. 1, no. 7, pp. 1-8, 2013.

[12]. R. Sanchez Zeferino, M. B. Flores and U. Pal, "Photoluminescence and Raman scattering in Ag-doped ZnO nanoparticles," J. Appli. Phys. vol. 109, pp. 308-312, 2011.

[13]. S. Roy, M. Triparna, T. shatarupa and P. Das, "Biosynthesis, characterization and antifungal activity of silver nanoparticles synthesized by the fungus Aspergillus foetidus," J. Nanometer. Biostruc. vol. 8, pp. 197–205, 2013.

[14]. T. C. N. Prathna, A. M. Chandrasekaran, A. Raichur and Mukherjee, "Biomimetic synthesis of silver nanoparticles by Citrus limon (Lemon) aqueous extract and theoretical prediction of particle size," Colloid. Surf. B: Bioint. vol. 82, pp. 152-159, 2011.

[15]. M. Forough and K. Farhadi, "Biological and green synthesis of silver nanoparticles," Turkish J. Eng. Env. Sci. vol. 34, pp. 281 – 287, 2010.

[16]. J. Mohammed, Haider and M. S. Mehdi, "Study of morphology and Zeta Potential analyzer for the silver nanoparticles," Int. J. Scienti. Engineer. Res. vol. 5, no. 7, pp. 381-387, 2014.

[17]. R. Chauhan, A. Kumar and R. P. Chaudhary, "Synthesis and characterization of silver doped ZnO nanoparticles," Arch. Appl. Sci. Res. vol. 2, no. 5, pp. 378–385, 2010.

[18]. D. Wang, Y. Yu, H. L. Xin, R. Hovden, P. Ercius, J. A. Mundy, H. Chen, J. H. Richard, D. A. Muller, F. J. Disalvo and H. D. Abruna, "Tuning oxygen reduction reaction activity via controllable dealloying: A model study of ordered Cu3Pt/C intermetallic nanocatalysts," Nano. Letters vol. 12, no. 10, pp. 5230-5238, 2012.

[19]. R. K. Shah, F. Boruah and N. Parween, "Synthesis and characterization of ZnO nanoparticles using leaf extract of Camellia sinesis and evaluation of their antimicrobial efficacy," Int. J. Curr. Microbiol. Appl. Sci. vol. 4, no. 8, pp. 444-450, 2015.

[20]. O. D. Jayakumar, V. Sudarsan, C. Sudakar, R. Naik, R. K. Vatsa and A. K. Tyagi, "Green emission from ZnO nanorods: Role of defects and morphology," Scr. Mater. vol. 62, pp. 662–665, 2010.

[21]. D. Guin, S. V. Manorama, J. N. L. Latha and S. Singh, "Photoreduction of silver on bare and colloidal TiO2nanoparticles/nanotubes: Synthesis, characterization, and tested for antibacterial outcome," J. Phys. Chem. C. vol. 111, pp. 13393-13397, 2007.

[22]. S. S. Patil, R. H. Patil, S. B. Kale, M. S., Tamboli, J. D., Ambekar, W. N., Gade, S. S., Kolekar and B. B. Kale, "Nanostructured microspheres of silver zinc oxide: Anexcellent impeder of

bacterial growth and biofilm," J. Nanoparticle Res. vol. 16, pp. 1–11, 2014.

[23]. L. Zung, L. Jiang and Y., Ding, "Investigation into antibacterial behaviour of suspensions of ZnO nanoparticles against Coli," J. Nanopart. Res. vol. 12, pp. 1625-1636, 2010.

[24]. S. Gayathri, O. S. N. Ghosh, S. Sathishkumar, P. Sudhakara, J. Jayaramudu, S. S. Ray and A. K. Viswanath, Investigation of physicochemical properties of Ag doped ZnO nanoparticles prepared by chemical route," Appl. Sci. Lett. Vol. 1 no. 1, pp. 8-13, 2015.

[25]. S. Y. Pung, W. P. Lee and A. Aziz, "Kinetic study of organic dye degradation using ZnO particles with different morphologies as a photocatalyst," Int. Inorg. Che. Vol. 3, pp. 1-9, 2012.

[26]. N. Nghia, N. N. K. Truong, N. M. Thong and N.P. Hung, "Synthesis of nanowire-shaped silver by polyol process of sodium chloride," Int. J. Mater. Chem. vol. 2, no. 2, pp. 75–78, 2012.

[27]. L. L. Zhang, Y. H. Jiang, Y. L. Ding, M. Povey and D. York, "Investigation into the antibacterial behavior of suspensions of ZnO nanoparticles," J. Nanopart. Res. vol. 9, pp. 479-489, 2007.

[28]. J. Mohammad, Hajipour, K. M. Fromm, A. A. Ashkarran, I. R. de Larramendi, T. Rojo, V. Serpooshan, W. J. Parak and M. Mahmoudi, "Antibacterial properties of nanoparticles," Trends Biotechnol. Vol. 30, pp. 10, 2012.

[29]. S. Jafarirad, M. Mehrabi, B. Divband and M. Kosari-Nasab, "Biofabrication of zinc oxide nanoparticles using fruit extract of Rosa canina and their toxic potential against bacteria: a mechanistic approach Mater," Sci. Eng. C. vol. 59, pp. 296–302, 2016.

[30]. K. Anandalakshmi, J., Venugobal and V. Ramasamy, "Characterization of silver anoparticles by green synthesis method using Pedalium murex leaf extract and their antibacterial activity," Appl. Nanosci. vol. 6, pp. 399, 2016.